ISSN 0001-4370, Oceanology, 2009, Vol. 49, No. 1, pp. 31–38. © Pleiades Publishing, Inc., 2009.
Original Russian Text © A.S. Zapevalov, A.N. Bol'shakov, V.E. Smolov, 2009, published in Okeanologiya, 2009, Vol. 49, No. 1, pp. 37–44.

Studying the Sea Surface Slopes Using an Array of Wave Gauge Sensors

A. S. Zapevalov, A. N. Bol'shakov, and V. E. Smolov

Marine Hydrographic Institute, National Academy of Science of Ukraine, ul. Kapitanskaya 2, Sevastopol, Crimea, 335000 Ukraine

Received January 23, 2008

Abstract—The deviations of the marine surface slope spectra (measured using an array of wave gauge sensors) from the theoretical estimates obtained using the linear spectral model of the wave field are analyzed. It has been indicated that the average measured full slope spectra (the sum of the slope component spectra in the orthogonal directions) is higher than the theoretical estimates by 6% at frequencies from the surface wave spectral peak (f_m) to $4.5 f_m$. The difference between the measured and theoretical estimates of the full slope spectrum rapidly increases at frequencies of $f < f_m$. At $f_m \approx 0.75 f_m$, the average measured full slope spectrum is higher than the theoretical estimate by a factor of more than 5.

DOI: 10.1134/S0001437009010044

INTRODUCTION

The works by Cox and Munk [10, 11], where the aerial survey of sun glints was used to determine the two-dimensional statistics of the longitudinal and transverse slope components relative to the wind direction, were the first significant experimental studies of undulating sea surface slopes. The method for determining sea surface slopes was based on the technique for estimating the slope values using the brightness distribution in solar and lunar glitter pattern [8].

At present, different types of equipment are used to measure sea surface slopes. Optical devices are used to study slopes generated by short waves. Laser slopemeters based on determining the deviations of a laser beam (crossing the undulated ocean–atmosphere boundary) from the vertical are used in addition to the above technologies, according to which slopes are determined by registering the light reflected from the sea surface [7]. Special wave gauge buoys of the pitch-and-roll type, with their bodies operating as sensors, are used to measure slopes generated by waves longer than 5 m [12, 13]. Slopes formed by waves of the decimetric range are, as a rule, measured using pairs of string wave gauges. These pairs are arranged so that the vectors joining the points for measuring surface elevations are mutually perpendicular [4].

The present work considers the method for determining sea surface slopes based on the surface elevation measured at three points located outside a straight line. The preliminary results of studying sea surface slopes in the Black Sea coastal zone are discussed.

AVERAGE AND LOCAL SEA SURFACE SLOPES

We introduce the following denotations: η is the sea surface elevation; $\varsigma_x = \partial\eta/\partial x$ and $\varsigma_y = \partial\eta/\partial y$ are the components of the sea surface local slopes. The term "true" is also used for local slopes [5]. Local slopes are generated by waves of all surface scales (from long gravitational to capillary waves).

Various problems related to radio and acoustic scattering require information about the slopes generated by decimetric and meter waves. Finite-difference schemes are used to measure these waves. Average, rather than local, sea surface slopes are determined when wire wave gauge sensors are used in measurements:

$$\xi_x = \frac{\eta(x + \Delta x/2, y) - \eta(x - \Delta x/2, y)}{\Delta x}, \tag{1}$$

$$\xi_y = \frac{\eta(x, y + \Delta y/2) - \eta(x, y - \Delta y/2)}{\Delta y}, \tag{2}$$

where Δx and Δy are the distances between sensors along the OX and OY axes, respectively. The relation between the average and local slopes is described by the following expressions [5]:

$$\xi_x = (\Delta x)^{-1} \int_{x - \Delta x/2}^{x + \Delta x/2} \zeta_x dx, \tag{3}$$

$$\xi_y = (\Delta y)^{-1} \int_{y - \Delta y/2}^{y + \Delta y/2} \zeta_y dy, \tag{4}$$

The spectra of the average (S_Δ) and local (S_L) slopes are connected by the following relationships:

$$S_{\Delta x}(k,\Delta x) = R_x(k,\Delta x) S_{Lx}(k), \quad (5)$$

$$S_{\Delta y}(k,\Delta y) = R_y(k,\Delta y) S_{Ly}(k), \quad (6)$$

where $k = 2\pi/\lambda$ is the wave number. The $R_x(k,\Delta x)$ and $R_y(k,\Delta y)$ transfer functions are described by the expressions

$$R_x(k,\Delta x) = \frac{\int \varphi(k,\theta) F_x(k,\theta,\Delta x)\cos^2\theta d\theta}{\int \varphi(k,\theta)\cos^2\theta d\theta}, \quad (7)$$

$$R_y(k,\Delta y) = \frac{\int \varphi(k,\theta) F_y(k,\theta,\Delta y)\sin^2\theta d\theta}{\int \varphi(k,\theta)\sin^2\theta d\theta}, \quad (8)$$

where $\varphi(k,\theta)$ is the spreading function satisfying the condition

$$\int_{-\pi}^{\pi} \varphi(k,\alpha) d\alpha = 1,$$

$$F_x(k,\theta,\Delta x) = \left[\frac{\sin(\pi(\Delta x/\lambda)\cos\theta)}{\pi(\Delta x/\lambda)\cos\theta}\right]^2,$$

$$F_y(k,\theta,\Delta y) = \left[\frac{\sin(\pi(\Delta y/\lambda)\sin\theta)}{\pi(\Delta y/\lambda)\sin\theta}\right]^2.$$

From expressions (7) and (8), it follows that the form of the transfer function depends on the dimensionless distance $\varepsilon = \Delta x/\lambda$ (or $\varepsilon = \Delta y/\lambda$) and the angular distribution function $\varphi(k,\theta)$. When transfer functions are calculated, it is assumed that the dispersion relation holds true for gravitational waves in deep water

$$\omega^2 = gk, \quad (9)$$

where ω is the cyclic frequency, and g is the free fall acceleration.

We now consider two limiting cases when the angular distribution is unidirectional or isotropic. If the wave field includes components propagating in one direction (for definiteness, we assume that all the components propagate along the *OX* axis), then $S_{\Delta y}(k,\Delta y) = S_{Ly}(k) = 0$, and $R_x = F_x$. The situation when the wave energy distribution is isotropic (i.e., $\varphi(k,\theta) = \text{const}$) is another limiting case. In this situation, the transfer function is independent of the direction ($R_x = R_y$).

INSTRUMENTATION AND MEASUREMENT CONDITIONS

The measurements were performed in the summer and autumn of 2006 at the oceanographic platform of the Marine Hydrophysical Institute. The platform is located in the Black Sea near the southern Crimea coast. The depth in the platform area is 30 m, which corresponds to the deep water condition typical of wind-induced waves and swell on the Black Sea.

Wire resistance wave gauges were used to determine the characteristics of the surface wave field. A bare wire section vertically crossing the water–air interface is a sensor of such a wave gauge with a frequency range of 0.05–40 Hz. The resolution varied from 0.5 to 2.5 mm depending on the diameter and applied type of primary resistance converters [6].

The wire sensors formed an array composed of six elements. A wave gauge array was installed on a boom oriented toward the open sea. The boom was mounted on the southeastern angle support of the platform with a diameter of 55 cm. The distance from the support to the nearest wave gauge sensor was not less than 5 m.

In the present work, the sea surface slopes were calculated using the data of the surface elevation measurements at three points. The six-element array of spaced wave gauge sensors was installed as follows: five sensors were located at vertices of a regular pentagon inscribed in a circle with a radius of 25 cm, and one more sensor was located at the circle center.

The selected location of the sensors (Fig. 1) makes it possible to obtain three types of triangles: the first type can, e.g., include sensors 1–2–3; the second type, sensors 3–5–6; and the third type, sensors 1–4–6. Five variants of each type of triangles correspond to this location of sensors. Since the wave gauge sensors are located along one straight line in the third situation, we will analyze only the first two types of triangles (1–2–3, 3–5–6).

The plane including three points outside a straight line $a(x_a;y_a;z_a)$, $b(x_b;y_b;z_b)$, and $c(x_c;y_c;z_c)$ is described by the equation

$$Ax + By + Cz + D = 0, \quad (10)$$

where $A = \begin{vmatrix} y_a & z_a & 1 \\ y_b & z_b & 1 \\ y_c & z_c & 1 \end{vmatrix}$; $\mathrm{B} = \begin{vmatrix} z_a & x_a & 1 \\ z_b & x_b & 1 \\ z_c & x_c & 1 \end{vmatrix}$; $\mathrm{C} = \begin{vmatrix} x_a & y_a & 1 \\ x_b & y_b & 1 \\ x_c & y_c & 1 \end{vmatrix}$;

$\mathrm{D} = \begin{vmatrix} x_a & y_a & z_a \\ x_b & y_b & z_b \\ x_c & y_c & z_c \end{vmatrix}$. The slopes determined according to expression (10) using the measurements of sea slope elevations at three points will be used in the further analysis.

FULL SPECTRUM OF SEA SURFACE SLOPES

In the scope of the wave field linear model, the spectrum of wave numbers and directions $\Psi(k,\alpha)$ is con-

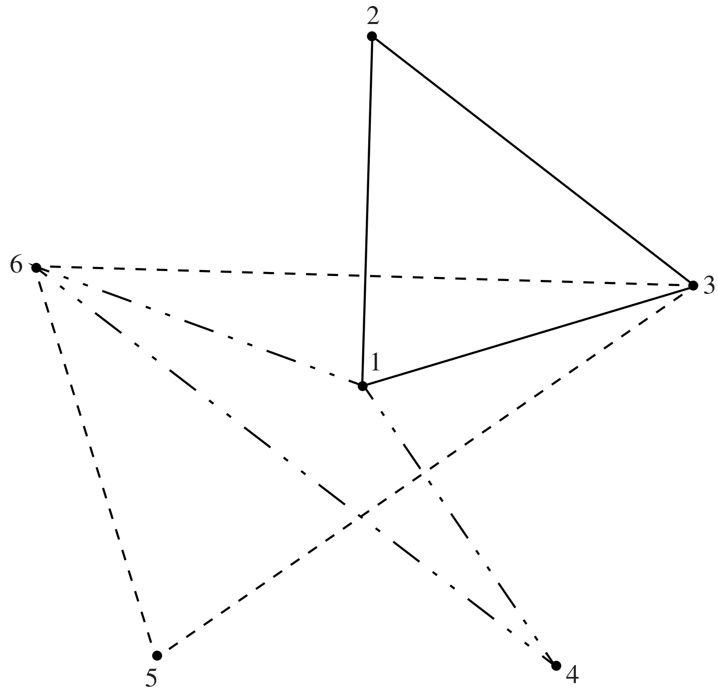

Fig. 1. Schematic location of wave gauge sensors.

nected to the spectra of two orthogonal components of local slopes by the integral relationships in the form

$$S_{Lx}(k) = \int_0^{2\pi} k^2 \cos^2\alpha \Psi(k, \alpha) d\alpha, \quad (11)$$

$$S_{Ly}(k) = \int_0^{2\pi} k^2 \sin^2\alpha \Psi(k, \alpha) d\alpha. \quad (12)$$

We now pass from the spectra determined in the wave number space to the frequency spectra. We define the full spectrum of sea surface slopes as

$$\chi_{L\Sigma}(\omega) = \chi_{Lx}(\omega) + \chi_{Ly}(\omega), \quad (13)$$

where $\chi_{Lx}(\omega)$ and $\chi_{Ly}(\omega)$ are the frequency spectra of the slope orthogonal components connected to the $S_{Lx}(k)$ and $S_{Ly}(k)$ spectra by the $\chi_{Lx}(\omega) = \frac{dk}{d\omega} S_{Lx}(k)$ and $\chi_{Ly}(\omega) = \frac{dk}{d\omega} S_{Ly}(k)$ relationships. The full slope spectrum $\chi_{L\Sigma}(\omega)$ generated by the linear field of gravitational waves satisfying the dispersion relation (9) is described by the expression

$$\chi_{L\Sigma}(\omega) = \frac{\omega^4}{g^2} s(\omega), \quad (14)$$

where $s(\omega)$ is the surface elevation spectrum.

We now compare the slope spectral characteristics determined during the experiment on the oceanographic platform to the characteristics following from the wave field linear model. Since the third wave gauge operated during not all the seances of measurements, its data were not analyzed. Thus, we considered the data on slopes obtained using three triangles of the first type (triangles 1–4–5, 1–5–6, 1–6–2) and two triangles of the second type (2–4–5 and 4–6–2, see Fig. 1). Hereafter, the first- and second-type triangles are called small and large triangles, respectively.

The spectral estimates of the sea surface slopes were obtained using the numerical series determined on a 10-min interval. The spectra were calculated using the Fourier transform method for the correlation functions [1]. Smoothing was performed using a Blackman–Tukey window. The calculations were conducted using smoothing with 128 degrees of freedom.

The behavior of the full slope spectra $\chi_{L\Sigma}$ obtained according to expression (14) and $\chi_{\Delta\Sigma}$ determined using the surface elevation measurements at three points is shown in Fig. 2. The $\chi_{\Delta\Sigma}$ spectrum was calculated as the sum of the slope orthogonal component spectra determined according to (10). When the data of measurements are analyzed, it is more convenient to operate with the spectral characteristics determined in the $f = \omega/(2\pi)$ region; therefore, we passed from the $s(\omega)$,

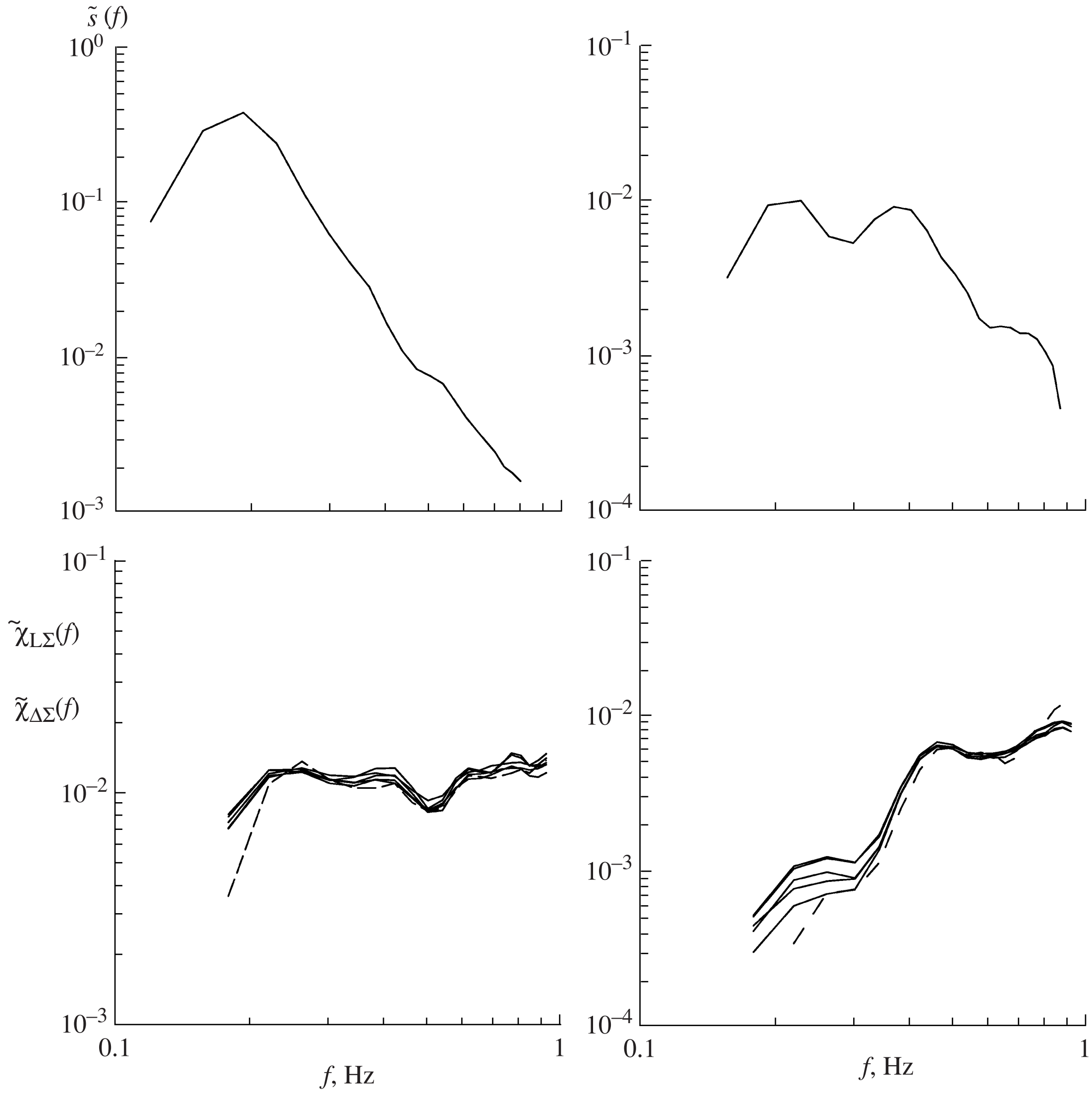

Fig. 2. Frequency spectra of the sea surface elevation $\tilde{s}(f)$ and the spectra of the local $\tilde{\chi}_{L\Sigma}(f)$ (dashed line) and average $\tilde{\chi}_{\Delta\Sigma}(f)$ (solid line) slopes. The results of the measurements in the situations when one and two wave systems were observed are presented in the left- and right-hand panels, respectively.

$\chi_{L\Sigma}(\omega)$, and $\chi_{\Delta\Sigma}(\omega)$ spectra to the $\tilde{s}(f)$, $\tilde{\chi}_{L\Sigma}(f)$, and $\tilde{\chi}_{\Delta\Sigma}(f)$ spectra. Figure 2 reflects the situations when one (left-hand panels) and two (right-hand panels) clearly defined wave systems were observed on the sea surface.

The full slope spectra $\tilde{s}(f)$ and the $\tilde{\chi}_{L\Sigma}(f)$ spectra almost coincide at frequencies higher than the peak frequency in the surface elevation spectrum $\tilde{\chi}_{\Delta\Sigma}(f)$ (denoted as f_m). Pronounced differences are observed in the $f < f_m$ region, where the measured values of the slope spectra $\tilde{\chi}_{\Delta\Sigma}(f)$ considerably exceed the spectra $\tilde{\chi}_{L\Sigma}(f)$ calculated using the linear model. In this case, all the estimates of the $\tilde{\chi}_{\Delta\Sigma}(f)$ spectra calculated at different configurations of the wave gauge arrangement are close to one another.

In the presence of two surface wave systems, the $\tilde{\chi}_{\Delta\Sigma}(f) \approx \tilde{\chi}_{L\Sigma}(f)$ equality is observed only at frequencies in the vicinity of the high-frequency (the second) peak of the surface elevation spectrum f_{mh} in the $f > f_{mh}$ region. The $f < f_{mh}$ > inequality $\tilde{\chi}_{\Delta\Sigma}(f) > \tilde{\chi}_{L\Sigma}(f)$ holds true in the $f < f_{mh}$ spectral region, including the frequency of the low-frequency peak of the surface elevation spectrum. A considerable scatter of the $\tilde{\chi}_{\Delta\Sigma}(f)$ spectral estimates, calculated based on the measurements performed by the wave gauges forming different triangles, is also observed in the $f < f_{mh}$ region.

Kalinin and Leikin [4] were among the first researchers who paid attention to the fact that the measured slope spectra $\tilde{\chi}_{\Delta\Sigma}(f)$ in the $f < f_m$ frequency region are considerably higher than the spectra calculated using the linear model. These authors assumed than this effect is caused by low-frequency instrumental noise. Later, a similar result was obtained in [3].

We should note that the $\tilde{\chi}_{\Delta\Sigma}(f)$ spectrum was considerably higher than the $\tilde{\chi}_{L\Sigma}(f)$ spectrum in the $f < f_m$ region during three independent experiments performed using different instrumentation. In addition, the methods for determining the $\tilde{\chi}_{\Delta\Sigma}(f)$ spectrum were different. In [3, 4], this spectrum was estimated based on measurements of the difference in the sea surface elevations in two orthogonal directions. In the present work, we calculate this spectrum using the surface elevation measurements at three points forming an irregular triangle. This makes it possible to assume that the considered effect is caused by physical factors rather than technical ones.

Let us consider the behavior of the

$$\varepsilon = \frac{\tilde{\chi}_{\Delta\Sigma}}{\tilde{\chi}_{L\Sigma}} \tag{15}$$

function depending on the dimensionless frequency $\Omega = f/f_m$. We analyzed 60 seances of measurements performed under the conditions when only one wave system was observed on the sea surface. The $\varepsilon(\Omega)$ functions were determined for each of five wave gauge configurations indicated above forming a large or small triangle. The average value of the $\bar{\varepsilon}(\Omega)$ function for each seance and the rms deviations from this value $\Delta\varepsilon(\Omega)$ were subsequently calculated.

Figure 3 indicates that the $\bar{\varepsilon}(\Omega)$ function values in the $1 \le \Omega \le 4.5$ region are close to unity. In this region, the average value of the $\bar{\varepsilon}(\Omega)$ function for all the seances of measurements and for the considered frequency region is 1.06, and the average $<\bar{\varepsilon}(\Omega)>$ value is 0.05. The $<\Delta\varepsilon(\Omega)>$ value is 1.03 in the $1 \le \Omega \le 1.5$ region and slightly increases (to 1.08) at $2 \le \Omega \le 4$. The insignificant increase in the deviation of the $<\bar{\varepsilon}(\Omega)>$ values from unity with increasing $<\bar{\varepsilon}(\Omega)>$ can be explained by the fact that the dispersion relation (9) is violated under marine conditions. This is, specifically, confirmed by the measurements of the surface wave phase velocities (see the review of these studies in [9]). Nevertheless, we can assume that the sea surface slope spectra in the $1 \le \Omega \le 4.5$ region are sufficiently adequately described in the scope of the wave field linear model.

In the $\Omega < 1$ region, the spectra of the measured slopes strongly differ from those of the slopes calculated according to the linear model: $\tilde{\chi}_{L\Sigma} \ll \tilde{\chi}_{\Delta\Sigma}$. At $\Omega \approx 0.75$, the average $\tilde{\chi}_{\Delta\Sigma}$ spectrum exceeds the theoretical estimate $\tilde{\chi}_{L\Sigma}$ by a factor of more than 5. This is probably related to the fact that the surface wave spectrum rapidly rolls off at frequencies lower than f_m; therefore, even insignificant deviations of the real wave field from the linear model result in considerable differences between the $\tilde{\chi}_{L\Sigma}$ and $\tilde{\chi}_{\Delta\Sigma}$ spectral estimates.

We should also note that the frequency–angle characteristics of the sea surface wave field are calculated in the scope of the linear model when the measurements are performed using wave gauge buoys of the pitch-and-roll type. The data of the sea surface slope measurements obtained in the present work indicate that it is necessary to additionally study the region of this model application in order to determine the function of the wave energy angular distribution. The same conclusion was previously drawn based on an analysis of the coherence loss in the field of sea surface waves [2].

At the distances between string wave gauges that were established between sensors during the analyzed experiment, the slope spectral characteristics near a frequency of 1 Hz should be affected by the transfer functions of the wave gauge array considered above. The average estimates of the parameter $\bar{\varepsilon}$ for each seance of measurements constructed as a function of the frequency f are presented in Fig. 4. The estimates of the function $\bar{\varepsilon}$ are strongly scattered; nevertheless, after averaging over 60 seances, it becomes evident that this function rapidly decreases near $f = 1$ Hz.

For comparison, we present in Fig. 4b the transfer function (R) calculated according to (7) for the isotropic wave field at two values of the differences between sensors typical of small and large triangles. The arithmetical mean lengths of the triangle sides (26.5 and 36.8 cm) are taken as characteristic distances. It is evident that the $<\bar{\varepsilon}(f)>$ function decreases with increasing f faster than is caused by the transfer function calculated according to the linear model. The $<\bar{\varepsilon}(f)>$ function additionally decreases due to a rapid loss of coherence in the field of sea surface waves [3].

CONCLUSIONS

At present, information about the characteristics of sea surface slopes generated by microwaves and meter waves is mainly obtained during measurements performed using an array of spaced string wave gauge sensors. The wave field spatial characteristics, including slopes, are calculated in the scope of the linear model.

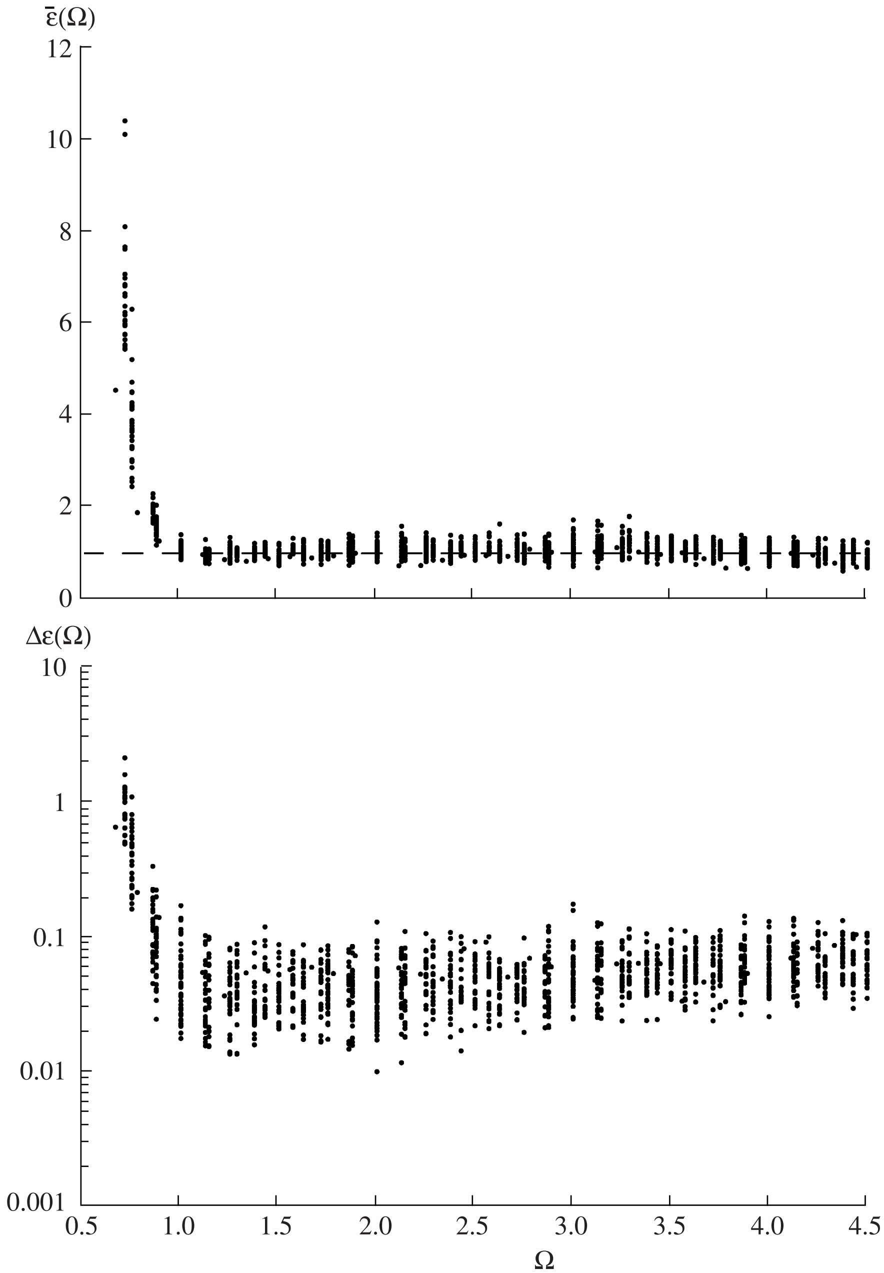

Fig. 3. The $\bar{\varepsilon}$ (Ω) and $\Delta\varepsilon(\Omega)$ functions of the $\Omega = f/f_m$ dimensionless frequency.

We analyzed the deviations of the full spectra of the sea surface slopes measured using an array of wave gauge sensors from the theoretical estimates obtained in the scope of the linear spectral model of the wave field. We considered two situations corresponding to the conditions when two and one wave systems were observed on the surface. In the first situation, the theoretical and experimental estimates of the slope spectra are close to each other only in the vicinity of the HF (the second) peak of the surface elevation spectrum (f_{mh}) and at $f > f_{mh}$.

In the situation when only one surface wave system is observed on the sea surface in the range from the peak frequency in the surface wave spectrum (f_m) to 4.5 f_m, the measured full slope spectra are higher than the theoretical estimates by 6% on average. The difference between the measured and theoretical estimates of the full slope spectrum rapidly increases at frequencies

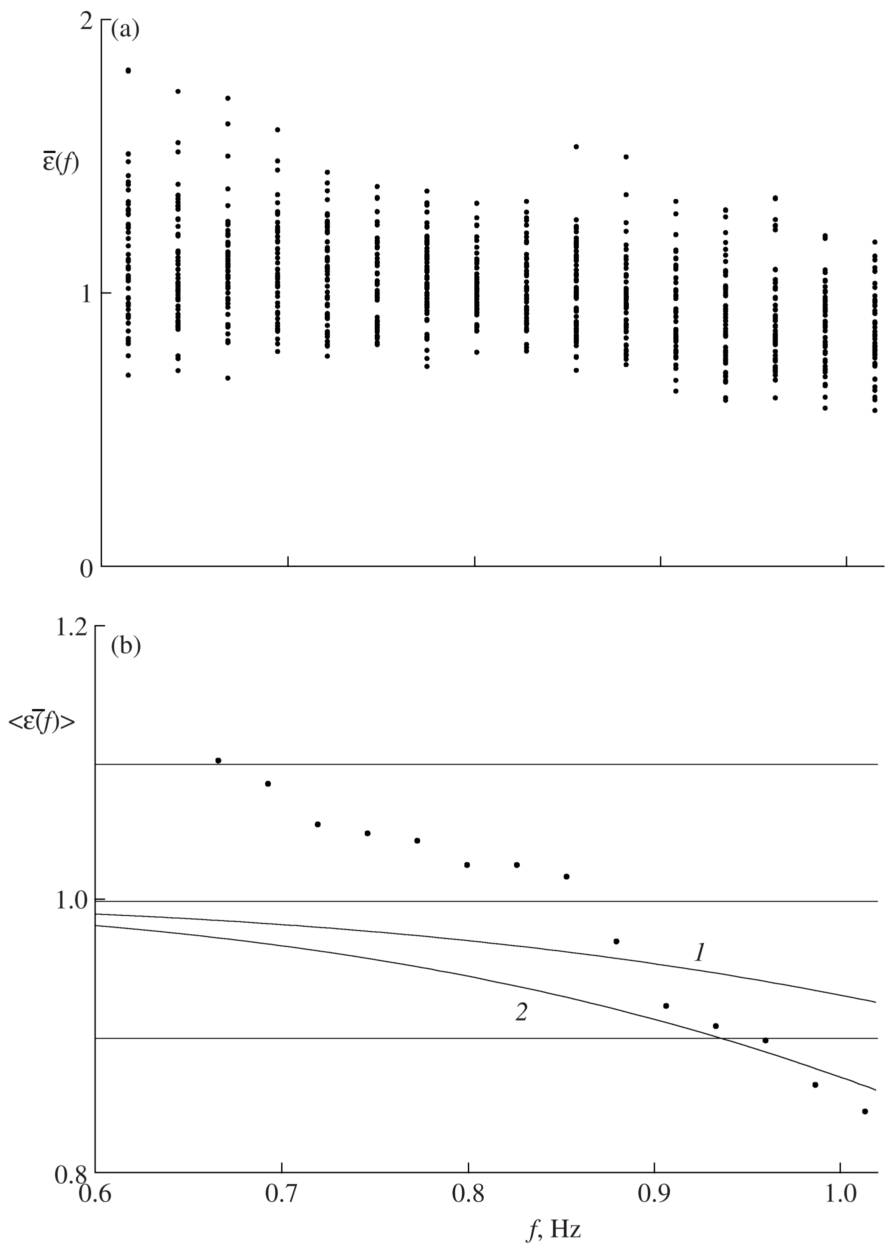

Fig. 4. Behavior of the (a) $\bar{\varepsilon}$ (f) and (b) $<\bar{\varepsilon}$ $(f)>$ functions when approaching a frequency of 1 Hz. Curves *1* and *2* correspond to the transfer function of a differential slopemeter in the isotropic wave field at distances of 26.5 and 36.8 cm between sensors, respectively.

$f < f_m$. At $f \approx 0.75 f_m$, the measured full slope spectrum is higher than the theoretical estimate by a factor of more than 5 on average.

REFERENCES

1. G. Jenkins and D. Watts, *Spectral Analysis and Its Applications* (Holden-Day, San Francisco, 1966; Mir, Moscow, 1972) [in Russian].
2. A. S. Zapevalov, "On Estimation of the Angular Distribution Function of the Dominant Sea Wave Energy," Izv. Akad. Nauk, Ser. Fiz. Atmos. Okeana **31** (6), 835–841 (1995).
3. A. S. Zapevalov and G. N. Khristoforov, "Transfer Function of a Differential Wave Gauge," Morskoi Gidrofiz. Zh., No. 2, 14–21 (1991).
4. S. A. Kalinin and I. A. Leikin, "Measurement of Wave Wind Slopes in the Caspian Sea," Izv. Akad. Nauk SSSR, Ser. Fiz. Atmos. Okeana **21** (2), 1210–1217 (1988).
5. G. V. Matushevskii, "Studying the Relation between True and Average Slopes of an Undulated Sea Surface,"

Izv. Akad. Nauk SSSR, Ser. Fiz. Atmos. Okeana **5** (4), 404–415 (1969).

6. V. E. Smolov and A. S. Zapevalov, "Differential Wave Gauge for Studying HF Field Components of Wind-Induced Sea Waves," in *Environmental Control Systems* (MGI NAN Ukrainy, Sevastopol, 2001), pp. 57–61 [in Russian].
7. G. N. Khristoforov, A. S. Zapevalov, and M. V. Babii, "Statistical Characteristics of Sea Surface Slopes at Different Wind Velocities," Okeanologiya **32** (3), 452–459 (1992).
8. V. V. Shuleikin, "Optical Method for Studying Sea Waves," Zap. Gidrogr. **5** (9), 49–56 (1924).
9. H. Yuen and B. Lake, *Nonlinear Dynamics of Deep-Water Gravity Waves* (Academic, New York, 1982; Mir, Moscow, 1987).
10. C. Cox and W. Munk, "Statistics of the Sea Surface Derived from the Sun Glitter," J. Mar. Res. **13** (2), 198–227 (1954).
11. C. Cox and W. Munk, "Measurements of the Roughness of the Sea Surface from Photographs of the Sun Glitter," J. Opt. Soc. Am. **44** (11), 838–850 (1954).
12. D. W. Wang and P. A. Hwang, "Evolution of Bimodal Directional Distribution of Ocean Waves," J. Phys. Oceanogr. **31**, 1200–1221 (2001).
13. D. W. Wang and P. A. Hwang, "Higher Fourier Harmonics of the Directional Distribution of an Equilibrium Wave Field Under Steady Wind Forcing," J. Atmos. Ocean. Technol. **20**, 217–227 (2003).